YTHDF3 modulates hematopoietic stem cells by recognizing RNA m^{6}A modification on *Ccnd1*

Xiaofei Zhang,[1*] Tingting Cong,[1*] Lei Wei,[2] Bixi Zhong,[2] Xiaowo Wang,[2] Jin Sun,[3] Shuxia Wang,[3] Meng Michelle Xu,[4] Ping Zhu,[3] Hong Jiang[5] and Jianwei Wang[1]

[1]School of Pharmaceutical Sciences, Tsinghua University, Beijing; [2]Ministry of Education Key Laboratory of Bioinformatics, Center for Synthetic and Systems Biology, Bioinformatics Division, BNRIST, Department of Automation, Tsinghua University, Beijing; [3]Department of Geriatrics, The Second Medical Center & National Clinical Research Center for Geriatric Diseases, Chinese PLA General Hospital, Beijing; [4]Department of Basic Medical Sciences, School of Medicine, Institute for Immunology, Beijing Key Lab for Immunological Research on Chronic Diseases, THU-PKU Center for Life Sciences, Tsinghua University, Beijing and [5]Kidney Disease Center, the First Affiliated Hospital, College of Medicine, Zhejiang University, Hangzhou, China

**XZ and TC contributed equally as co-first authors.*

Correspondence:
Ping Zhu
zhuping301hospital@163.com
Hong Jiang
jianghong961106@zju.edu.cn
Jianwei Wang
jianweiwang@mail.tsinghua.edu.cn

Received: July 30, 2021.
Accepted: November 25, 2021.
Prepublished: February 3, 2022.

https://doi.org/10.3324/haematol.2021.279739

Supplemental information

YTHDF3 modulates hematopoietic stem cells by recognizing RNA m^{6}A modification on *Ccnd1*

Xiaofei Zhang[1#], Tingting Cong[1#], Lei Wei[2], Bixi Zhong[2], Xiaowo Wang[2], Jin Sun[3], Shuxia Wang[3], Meng Michelle Xu[4], Ping Zhu[3*], Hong Jiang[5*], Jianwei Wang[1*]

[1]School of Pharmaceutical Sciences, Tsinghua University, Beijing 100084, China.

[2]Ministry of Education Key Laboratory of Bioinformatics, Center for Synthetic and Systems Biology, Bioinformatics Division, BNRIST, Department of Automation, Tsinghua University, Beijing, China

[3]Department of Geriatrics, The Second Medical Center & National Clinical Research Center for Geriatric Diseases, Chinese PLA General Hospital, 28 Fuxing Road, Beijing, China

[4]Department of Basic Medical Sciences, School of Medicine, Institute for Immunology, Beijing Key Lab for Immunological Research on Chronic Diseases, THU-PKU Center for Life Sciences, Tsinghua University, Beijing, China

[5]Kidney Disease Center, the First Affiliated Hospital, College of Medicine, Zhejiang University 310003, China

[#]These authors contribute equally

*Correspondence:zhuping301hospital@163.com;jianghong961106@zju.edu.cn; jianweiwang@mail.tsinghua.edu.cn

Additional Discussion

YTHDF3 is one of the readers deciphering m^{6}A signal in HSCs

In this study, we observed that *Ythdf3*$^{-/-}$ mice developed normally except for the increased number of HSCs (Fig.1D, 1F, 1I, 1J and S1H), suggesting that *Ythdf3* might be dispensable for the development and steady stage homeostasis of hematopoietic system. Another possibility is that *Ythdf3* might be compensated by other m^{6}A readers during embryonic stage.

Given that *Ythdf3*$^{-/-}$ HSCs recapitulated, but not as dramatic as, the phenotype of *Mettl3*$^{-/-}$ HSCs, and that the phenotype of *Ythdf1*$^{-/-}$ and *Ythdf2*$^{-/-}$ HSCs is not consistent with *Mettl3*$^{-/-}$ HSCs. It is conceivable that *Ythdf3* is one of the readers decoding m^{6}A signal in HSCs, while other m^{6}A readers may also exert their function in modulating HSC function by decoding m^{6}A modification. For example, *Ythdc1* can mediate nuclear export and splicing of m^{6}A mRNA,[34-35] and *Ythdc2* can enhance the translation efficiency of its targets and decrease their mRNA abundance.[36] It is possible that *Ythdc1* and *Ythdc2* modulate HSC function by reading m^{6}A signal.

In addition, a recent study has revealed that METTL3 deposits m^{6}A modifications on chromosome-associated regulatory RNAs (carRNAs) and these carRNAs can globally tune chromatin state and transcription in the nucleus.[37] However, *Ythdf3* is a cytoplasmic protein,[38] which may be one of the reasons for the phenotypic differences between *Ythdf3*$^{-/-}$ and *Mettl3*$^{-/-}$ mice.

Myc is the target of METTL3 to regulate HSC differentiation, but not reconstitution capacity

Two recent studies reported that *Mettl3* regulates *Myc*[17-18] and dysfunction of *Myc* severely impairs the self-renewal and differentiation capacity of HSCs,[39] which

recapitulates the phenotype of *Mettl3* deficient HSCs. Lee et al. revealed that enforced *Myc* rescues the differentiation defect of *Mettl3*$^{-/-}$ HSCs.[17] In our functional assays (Fig. 6I-J), we indeed observed that overexpression of MYC rescue the differentiation bias and donor-derived chimera of *Mettl3*-compromised LSK at the first month after transplantation, but the chimera dropped rapidly at the 2nd and 3rd months (Fig. 6I). The possible explanation is that enforced *Myc* rescued the differentiation bias of *Mettl3*-compromised LSKs, but did not benefit the self-renewal capacity of *Mettl3*$^{-/-}$ HSCs. Consistent with this explanation, Reavie et al. generated *Myc*$^{eGFP/eGFP}$ mice to study the dosage-effect of MYC on HSCs, and they observed that the self-renewal capacity of *Myc*^{hi}-HSCs is impaired.[40] Briefly, these studies suggest that overexpression of MYC is not able to rescue the self-renewal capacity of *Mettl3* deficient HSCs.

Ccnd1 is one of the METTL3 targets to regulate the reconstitution capacity of HSCs

Our study revealed that YTHDF3 regulates the translation of *Ccnd1* by recognizing m^{6}A modification at the 5'UTR of *Ccnd1*, wherein METTL3 "writes" m^{6}A modification. Furthermore, we identified two m^{6}A motifs (-180~-184, GGATC) and (-102~-106, AGACT) at the 5'UTR of *Ccnd1* (Fig. 3F-G, S4B and S4E). Consistently, Hirayama et al. reported that -180~-184 in the 5'UTR of *Ccnd1* is a RNA m^{6}A motif.[27] In addition, Meyer et al. revealed that a single mutation in m^{6}A motif is sufficient to alter protein translation.[41] In brief, these data suggest that the two m^{6}A motifs in the 5'UTR of *Ccnd1* are the key hubs for METTL3 and YTHDF3 to

transmit m^{6}A signal to modulate the expression of CCND1 (Fig. 3A, 3D, 5B and S6D). It is notable that enforced CCND1 completely rescued the reconstitution capacity of *Ythdf3*$^{-/-}$ HSC, but partially rescued *Mettl3*-compromised HSCs (Fig. 4D and 6G), indicating that there might be unidentified m^{6}A targeted genes regulating HSC function.

Two recent studies conducted m^{6}A modification profile in HSCs and hematopoietic progenitor cells[17-18], although *Ccnd1* is not detected in such assays, the possible reason is that the low number of HSCs limits the accuracy of m^{6}A sequencing. The development of more sensitive m^{6}A sequencing technology may be able to identify more m^{6}A targets regulating HSCs function. Regarding the downstream pathway that *Ccnd1* modulates HSC function, Chaves-Ferreira et al. found that the carboxyl regulatory domain of CCND1 is the key region to regulate the differentiation and reconstitution capacity of HSCs.[42] Choi et al. reported that D-cyclins, including *Ccnd1/2/3*, inhibits apoptosis pathway by controlling death receptor Fas and FasL.[43] It is conceivable that cell death signaling might be the target of *Ccnd1* to modulate HSC function.

In conclusion, our study for the first time elucidated how m^{6}A reader YTHDF3 regulates HSC function. This study provides an important reference for exploring the mechanism of RNA m^{6}A modification and other RNA modifications to regulate the function of HSC and other somatic stem cells.

Supplemental Methods

Mice

Rosa26-LSL-Cas9 knockin mice (*Cas9*$^{+/+}$ GFP mice) were purchased from the Jackson Laboratory. To achieve hematopoietic-specifically expressed *Cas9* mice, *Cas9*$^{+/+}$ GFP mice were crossed to *Vav1-cre* mice. *Mettl3*$^{fl/fl}$ (C57BL/6N-*Mettl3*^{em1cyagen}) mice were generated by inserting loxP sites spanning the second and third exon of *Mettl3* via homologous recombination (Fig. 5A). *Ythdf1*-deficient (C57BL/6N-*Ythdf1*^{em1cyagen}) and *Ythdf3*-deficient (C57BL/6N-*Ythdf3*^{em1cyagen}) mice on C57BL/6 N background were generated using CRISPR-Cas9 system (Fig. 1A and 1B). In brief, a mixture of Cas9 protein and sgRNAs were injected into fertilized eggs, which then were planted into pseudopregnant mice. Mouse genomic DNA was extracted from the tails of 3-week-old mice using phenol-chloroform and recovered by alcohol precipitation to detect the third exon deletion of *Ythdf1 or Ythdf3*. To induce Cre expression in *Mx1*-cre; *Mettl3*$^{fl/fl}$ mice, mice were intraperitoneally injected with pIpC (12.5mg/kg) every other day for five times. All of these strains were maintained on C57BL/6 background. All genotyping primers were listed in Table S1.

Lentivirus Production and Transduction

The mouse *Ccnd1* and *Myc* were cloned into pRRL-PPT-SF-newMCS-IRES2-EGFP vector and pRRL-PPT-SF-newMCS-IRES2-mCherry Vector. The *Ythdf3, Mettl3, Pabpc1* and *Eif4g2* shRNAs were cloned into SF-LV-miRE-EGFP vector. The *Ccnd1* gRNAs were cloned into SF-LV-gRNA-mCherry vector. Lentivirus was produced in 293T cells and was concentrated according to standard procedures. For lentiviral transduction, LSK (cKit^{+} Sca1^{+} Lineage^{-}) cells were sorted and plated in 100 μl

SFEM medium (Stem Cell Technology, 09650) with 20ng/mL mSCF, 20ng/mL mTPO and 1 % penicillin/streptomycin in 96-well plate (~1×10^5 per well).

Construction of Plasmids

For *Ccnd1* 5'UTR and 3'UTR reporter vector, a 136bp and 232bp 5'UTR mRNA sequence upstream of *Ccnd1* translation start site were cloned into pGL3 Basic vector. *Ccnd1*-5'UTR-WT1-F (TCTATCGATAGGTACTTTTCTCTGCCCGGCTTTGAT) and *Ccnd1*-5'UTR-WT2-F (TCTATCGATAGGTACCAGGGGAGTTTTGTTGAAGTTGC) which introduced 15bp homologous base sequence upstream of pGL3 Basic vector *Kpn* I site and *Ccnd1*-5'UTR-WT1-R (GATCTCGAGCCCGGGCGCGGAGTCTGTAGCTCTCT) and *Ccnd1*-5'UTR-WT2-R (GATCTCGAGCCCGGGGGCGCGGCCGTCTGGGGA) which introduced 15bp homologous base sequence downstream of pGL3 Basic vector *Nhe* I site. According to the instruction of TIANGEN EasyGeno Assembly Cloning Kit, the PCR product and pGL3 Basic vector were double digested with *Kpn* I and *Nhe* I, and yield the pGL3-*Ccnd1*-5'UTR-WT1 vector and pGL3-*Ccnd1*-5'UTR-WT2 vector. By using the similar method, a 1124bp 3'UTR mRNA sequence downstream of *Ccnd1* stop codon were cloned into psiCHECK2 vector. *Ccnd1*-3'UTR-WT1-F (ATTCTAGGCGATCGCTTTTGTTGGGTCAAGAAGAGAGAAC) which introduced 15bp homologous base sequence upstream of psiCHECK2 vector *Xho* I site and *Ccnd1*-3'UTR-WT1-R (TTTATTGCGGCCAGCCAACAGGCCGCTACAAGAAACAA) which introduced 15bp homologous base sequence downstream of psiCHECK2 vector *Not* I site. And

we acquired psiCHECK2-*Ccnd1*-3'UTR-WT1 vector.

To mutate the predicted binding sites of RNA m^6A on *Ccnd1* mRNA, *Ccnd1*-5'UTR-mut1-F (5'- AGTAACGTCACACGGGCTACAGGGGAGTTTTGTTGAAG -3') and *Ccnd1*-5'UTR-mut1-R (5'- CCCGTGTGACGTTACTGTTGTTAAGCAGAGATCAAAG -3') were used to convert A into G; *Ccnd1*-5'UTR-mut2-F (5'- AGCAGAGAGCTACAGGCTCCGCGCGCTCCGGAGAC -3') and *Ccnd1*-5'UTR-mut2-R (5'- CCTGTAGCTCTCTGCTACTGCGCCGACAGCCCTCTG -3') were used to convert A into G; *Ccnd1*-3'UTR-mut1-F (5'- TGAGGAAAATTAGGGGGCTCCAAAAGAGTTTGATTC -3') and *Ccnd1*-3'UTR-mut1-R (5'- CCCCCTAATTTTCCTCAGTTTGGATGGCTCTCCAATG -3') were used to convert A into G; *Ccnd1*-3'UTR-mut2-F (5'- TGTGCCTTTCTATTAGGGCTTTTTGGCAGAAGGTGGA -3') and *Ccnd1*-3'UTR-mut2-R (5'- CCCTAATAGAAAGGCACAGAGCCAGAGGTGTGCAAATT -3') were used to convert A into G. To overexpress *Ythdf3*, we cloned the CDS of *Ythdf3* into pRRL-PPT-SF-newMCS-IRES2-EGFP vector by using the following primers: forward: 5′- GACAGACTAGTTCGACGCGTATGTCAGCCACTAGCGTGGA-3′which introduced 15bp homologous base sequence upstream of pRRL-PPT-SF-newMCS-IRES2-EGFP vector *Mlu* I site, and reverse: 5′-GGAGGGAGAGGGGCGGATCCTTATTGCTTGTTTCTATTTCTCTCCC-3′ which introduced 15bp homologous base sequence downstream of pRRL-PPT-SF-newMCS-IRES2-EGFP vector *BamH* I site. Similarly, the *Mettl3* overexpressed vector was

constructed with the primers *Mettl3*-F (5'-GACAGACTAGTTCGACGCGTATGTCGGACACGTGGAGCTCT -3') and *Mettl3*-R (5'-GGAGGGAGAGGGGCGGATCCCTATAAATTCTTAGGTTTAGAGATGATGC -3'). The mutation of *Mettl3* (D395A) and *Ythdf3* (W438A, W492A) was also cloned into pRRL-PPT-SF-newMCS-IRES2-EGFP vector. For Co-immunoprecipitation assay, *Ythdf3*, *Pabpc1* and *eIF4G2* CDNAs were subcloned into the pDONR201 vector (Invitrogen) as entry clones and were subsequently transferred to gateway-compatible destination vectors for the expression of N- or C-terminal-tagged fusion protein.

Luciferase Assay

For the report gene experiments of *Ccnd1*-5'UTR, 293T cells were transfected with pGL3-*Ccnd1*-WT1 vector or pGL3-*Ccnd1*-mut1 vector and OE-*Ythdf3* vector, OE-*Mettl3* vector, the negative control vector using Lipofectamine 2000 after growing at approximately 70% confluence. Similarly, pGL3-*Ccnd1*-WT2 vector and pGL3-*Ccnd1*-mut2 vector were treated in the same way. For the report gene experiments of *Ccnd1*-3'UTR, 293T cells were transfected with psiCheck2- *Ccnd1*-WT1 vector or psiCheck2-*Ccnd1*-mut1 vector and OE-*Ythdf3* vector, OE-*Mettl3* vector, the negative control vector using Lipofectamine 2000 after growing at approximately 70% confluence. Similarly, psiCheck2-*Ccnd1*-WT1 vector and psiCheck2-*Ccnd1*-mut2 vector were treated in the same way. Among all the assays above, luciferase assays were performed by Dual-Luciferase Reporter Assay System (Promega, Madison, WI, USA) according to the manufacturer's instructions after the cells were transfected 48

hours. For the report gene experiments of *Ccnd1*-5'UTR were normalized to Renilla luciferase activity and for the report gene experiments of *Ccnd1*-3'UTR were normalized to firefly luciferase activity. All experiments were performed in triplicate.

Short-Term Homing Assay

Ythdf3$^{-/-}$ or WT (CD45.2) Lin^{-} Sca1^{+} donor cells (2×10^4 cells per recipient mouse) were transplanted by tail-vein injection into lethally irradiated recipient mice (CD45.1/2). The absolute number of donor-derived cells (CD45.2^{+} Lin^{-} Sca1^{+}) in the recipient's BM (2 femurs) of recipient mice was analyzed and calculated after 24 h transplantation. Percent homing efficiency is calculated by the absolute number of CD45.2^{+} Lin^{-} Sca1^{+} cells in the recipient's BM (2 femurs) divided by the number of transplanted donor cells (2×10^4 cells).

Blood Cell Counts

Mice were bled and analyzed using an Auto Hematology Analyzer BC-5000 (MINDRAY).

Transplantations and Peripheral Blood Analysis

Recipient mice were administered a lethal dose of radiation (10Gy) using X-ray irradiator (RS-2000, Rad Source Technologies) prior to transplantation. Recipient mice were administered with antibiotic water for 2-3 weeks following transplantation, and analyzed for donor-derived chimaerism (including myeloid, B and T cells) every month. The antibodies used to analyze peripheral blood chimaerism were listed in Table S2.

Quantitative Real-time PCR

Total RNA was extracted using TRIzol (Thermo Fisher Scientific) according to the manufacturer's instructions. Total RNA was subjected to reverse transcription using Revert Aid First Strand cDNA Synthesis Kit (Takara, RR047A) with random primers. Quantitative real-time PCR was performed on QuantStudio-3 Real-time PCR System (Applied Biosystems) using the 2× SYBR Green master mix (Applied Biosystems). The primer information is listed in Table S1.

RNA Library Preparation and Sequencing

The transcriptome sequencing was performed by ANNOROAD Gene Technology Company. First, 30 donor-derived HSCs (Lin^- $Sca1^+$ $cKit^+$ $CD34^-$ $CD150^+$) from *Ythdf3*$^{-/-}$ mice were sorted into lysis buffer directly. The transcriptome libraries were prepared using Smart-seq2 method. Then, Agilent Bioanalyzer 2100 system (Agilent Technologies) was used to assess the insertion size, and HiSeq PE Cluster Kit v4-cBot-HS (Illumina) was used to perform the clustering of the index-coded samples according the manufacturer's instructions. Finally, the libraries were sequenced using an Illumina Hiseq platform with 150-bp paired-end.

RNA immunoprecipitation followed by quantitative real-time PCR (RIP-qPCR)

2×10^7 3T3 cells were crosslinked at 254 nm UV light with 600 mJ/cm^2 and lysed in ice-colded lysis buffer (50 mM Tris–HCl pH 7.4, 150 mM NaCl, 1% Triton X-100, 5% glycerol, supplemented with 1 mM DTT, 1 mM PMSF, 1:500 PI cocktail and 400 U/ml RNase Inhibitor) for 30 min. The cell lysates were treated with DNase I for 10 min and 5% of the cell lysate was saved as input for RT-qPCR. The lysate was incubated with 4 μg YTHDF3 antibody (Abcam, ab220161), METTL3 antibody

(Proteintech, 15073-1-AP), eIF4G2 (Cell Signaling Technology, 3468S), PABPC1 (Proteintech, 10970-1-AP), m^6A-antibody (New England Biolabs, E1611A) or same amount of IgG (Cell Signaling Technology) at 4°C overnight. 25 μL Protein A/G beads (Santa, sc-2003, pre-equilibrated with 5 μg/mL yeast tRNAs) were added and incubated for another 2 h. The beads were washed with 500 μl RIP200 buffer (20mM Tris-Cl pH7.4, 200mM NaCl, 1mM EDTA, 0.3 TritonX-100, 5% glycerol) for four times at 4°C, 5-10min per wash. The RNA/protein complex was eluted by Proteinase K digestion buffer (containing 20ug Pronteinase K, 50mM Tris 7.4, 150mM NaCl, 0.5% SDS, 5mM EDTA, proteinase K was added freshly). The RNA was extracted by TRIzol™ Reagent (Invitrogen) according to the manufacturer's protocol. Reverse transcription was performed using Revert Aid First Strand cDNA Synthesis Kit (Takara, RR047A) with random primers. Quantitative real-time PCR was performed on QuantStudio-3 Real-time PCR System (Applied Biosystems) using the 2× SYBR Green master mix (Applied Biosystems). The enrichment of RIP-qPCR was normalized to IgG control.

Co-immunoprecipitation and Western Blotting

For transient transfection and co-immunoprecipitation assays, constructs encoding SFB-tagged and Myc-tagged proteins were transiently co-transfected into HEK293T cells. The transfected cells were lysed with NETN buffer (20 mM Tris-HCl, pH 8.0, 100 mM NaCl, 1 mM EDTA, and 0.5% Nonidet P-40) containing 20 mM NaF, and 1 mg/mL of pepstatin A and aprotinin on ice for 20 min. After removal of cell debris by centrifugation, the soluble fractions were collected and incubated with S-protein

beads for 4 hr at 4°C. Beads were washed three times with NTEN buffer, boiled in 2× SDS loading buffer, and resolved on SDS-PAGE. Membranes were blocked in 5% milk in tris-buffered saline (TBS) and Tween 20 (TBST) buffer and then probed with antibodies as indicated. For NIH/3T3 (3T3) and HEK/293T (293T) cells, NIH/3T3 (3T3) and HEK/293T (293T) cells were isolated and lysed with 120 μL NETN buffer (20 mM Tris-HCl, pH 8.0, 100 mM NaCl, 1 mM EDTA, 0.5% Nonidet P-40, containing protease and phosphatase inhibitors cocktail) on ice for 30 min and then centrifuged at 12000 rpm for 10 min. The supernatant was collected and then boiled with 2×Loading buffer. For LSK cells, freshly isolated LSK ($cKit^+$ $Sca1^+$ $Lineage^-$) cells were lysed in SDS loading buffer, lysis was completed by sonication and denatured by boiling. Samples were resolved on 10% SDS-PAGE. Membranes were blocked with 5% milk in TBST buffer and then probed with indicated primary antibodies.

Flow Cytometric Analysis and Cell Sorting

Bone marrow cells were harvested by crushing the bones (femurs, tibias and pelvis) with pestle and mortal in HBSS with 2% fetal bovine serum and 1% HEPES buffer ($HBSS^+$). Viable cells were counted by Vi-CELL XR Cell Viability Analyzer (Beckman Coulter). Cells were stained with antibodies labeled with fluorochromes (Table S2). Hematopoietic populations (Table S2) were identified by flow cytometry using BD LSR Fortessa (BD Biosciences, San Jose, CA). BD Influx (BD Biosciences) was used to purify cells. FACS data were analyzed using FlowJo software (TreeStar, Ashland, OR).

Protein synthesis assays

Click-iT assays were performed using WT or *Ythdf3*$^{-/-}$ LSK (cKit^{+} Sca1^{+} Lineage^{-}) cells (~1.5 × 10^{5} per well). O-propargyl-puromycin (OPP; 20 μM) (Life Technologies) was added to the cells and incubated for 30 minutes. Cells were washed in ice-cold PBS and then fixed and permeabilized using the Cytofix/Cytoperm Fixation Permeabilization Kit (BD Biosciences). Alexa-Fluor (Life Technologies) was conjugated to OPP as described in the manufacturer's instructions. Cells were washed in Cytoperm buffer (BD Biosciences) and resuspended in fluorescence-activated cell sorting buffer before data acquisition using BD LSR Fortessa (BD Biosciences, San Jose, CA). As a positive control, a well of cells were treated with 100μg/ml cycloheximide which can inhibit protein synthesis and OPP, and as a negative control, PBS was added to cells instead of OPP. Data analysis was performed using FlowJo Software (Becton, Dickinson and Company).

Cell cycle assay

For HSC cycle analysis, 2×10^{6} c-Kit^{+} cells were enriched and stained with relative surface markers (CD34^{-} LSK), then fixed for 15min, washed and permed along with intracellular Ki67 staining for 30min by using FIX and PERM® Cell Fixation & Permeabilization Kit (Invitrogenused, GAS004) and Ki67-FITC (BD Biosciences,558616), then stained with 50μg/mL DAPI (Sigma, D8417).

Cell apoptosis assay

Freshly isolated LSKs from WT or *Ythdf3*$^{-/-}$ were cultured for 24h in StemSpan serum-free medium (SFEM) (Stem Cell Technologies, #09650, Vancouver, Canada)

supplied with 20ng/mL mTPO (Peprotech, 315–14), 20ng/mL mSCF (Peprotech, 250–03) and 50U/mL penicillin/streptomycin (Hyclone, SV30010). All cells were cultured at 37°C with 5% CO_2. Then washed and stained with Annexin V-FITC (BD Biosciences, 556420) and Propidium iodide (MCE, #HYD0815/CS-7538) according to the product introduction, the cells were identified by flow cytometry using BD LSR Fortessa (BD Biosciences, San Jose, CA).

RNA Sequencing Data Analysis

The trimmed RNA sequencing reads were mapped to the mouse reference mm10 from UCSC database through hisat2 (v2.2.1).[44] Then, the reads were quantified by HTSeq (v0.12.4).[45] The prcomp function in R was used to do principal component analysis (PCA) with the raw sequencing counts. R package DESeq2 (v1.0) was used to analyze differentiate expression levels of samples between knockout and wildtype groups. The genes were ranked with the statistic value of DESeq2, and then were analyzed with GSEA (Gene Set Enrichment Analysis, v4.1.0) software[46] with the PreRanked weighted mode. HSC fingerprint genesets used for GSEA were collected from literatures[47] and the gene lists were shown in Supporting Information Table S3.

Statistical analysis

Statistical analysis was made using the Prism software (Prism, GraphPad Software Inc., San Diego, CA USA). Data are shown as mean ± SEM. Student's t test (Two-tailed unpaired) were used for comparisons (GraphPad Prism 7.0; ns, not significant). All experiments were repeated twice or three times independently.

Supplementary Tables Legends

Table S1, primers supplemental. (see excel file)

Table S2, materials supplemental. (see excel file)

Table S3, HSC fingerprint genes supplemental. (see excel file)

Supplementary Figures Legends

Figure S1. Dysfunction of *Ythdf3*, but not *Ythdf1*, mildly disturbs the hematopoietic system

(A) Bone marrow cells per femur (N= 6 mice per group. Data are shown as mean ± SEM).

(B-C) The scatter plot depicts the absolute number of CMPs, GMPs, MEPs, CLPs, MPPs (B) and HSCs (C) between WT and *Ythdf1*$^{-/-}$ mice (2 months old). N = 6 mice per group. Data are shown as mean ± SEM.

(D) Bone marrow cells per femur (N = 6 mice per group. Data are shown as mean ± SEM).

(E-F) The scatter plot depicts the absolute number of CMPs, GMPs, MEPs, CLPs, MPPs (E) and HSCs (F) between WT and *Ythdf3*$^{-/-}$ mice (2 months old). N = 6 mice per group. Data are shown as mean ± SEM.

(G-H) The scatter plots depict the percentage of myeloid, B and T cells in bone marrow cells between WT and *Ythdf1*$^{-/-}$ mice (G), WT and *Ythdf3*$^{-/-}$ mice (H) (2 months old). N=6 mice per group. Data are shown as mean ± SEM.

(I-J) The scatter plots depict the percentage of T cells in thymus (I) and spleen (J) between WT and *Ythdf3*$^{-/-}$ mice (2 months old). N=5 mice per group. Data are shown as mean ± SEM.

(K-L) Representative flow cytometry plots (K) and the scatter plots (L) display the cell cycle analysis of WT and *Ythdf3*$^{-/-}$ HSCs (CD34^{-} LSK). N=4-5, data are shown as mean ± SEM.

Figure S2. The reconstitution capacity of *Ythdf3*-deficient HSCs is impaired

(A-B) The scatter plots display the lineage distribution of myeloid cell, B cell and T cell among donor-derived cells between WT and *Ythdf1*$^{-/-}$ mice (A), WT and *Ythdf3*$^{-/-}$ mice (B) in peripheral blood at the end of the 4th month after transplantation. N=5

mice per group. Data are shown as mean ± SEM.

(C-D) Representative flow cytometry plots depict the gating strategy (C) and the percentage of donor-derived HSCs ($CD34^-$ $CD150^+$ LSK) in WT or *Ythdf3*$^{-/-}$ recipients at the 4^{th} month after transplantation (D). N=5 mice per group. Data are shown as mean ± SEM.

(E) Freshly isolated WT LSKs were infected by lentivirus carrying *Ythdf3* shRNAs or control. 72 hours later, 20,000 GFP^+ cells were purified and transplanted into lethally irradiated recipients together with 2.5×10^5 competitor cells. Engraftment was determined by donor derived GFP^+ cell in B ($B220^+$), T ($CD3^+$) and myeloid ($Mac\text{-}1^+$) cell every month after transplantation. N=6-7 per group. Data are shown as mean ± SEM. The gating strategy to generate these line plots are presented in Fig. S5G.

(F) This PCA (principal component analysis) plot shows the classification of *Ythdf3*$^{-/-}$ HSCs and WT HSCs based on the normalized RNA-seq levels of all mouse genes.

(G) The figure shows the Gene set enrichment analysis (GSEA) of apoptosis-related genes between *Ythdf3*$^{-/-}$ and WT HSCs. NES, normalized enrichment score. |NES|>0.3 and $p<0.05$ represent significant difference.

(H-J) Freshly isolated LSK cells of WT or *Ythdf3*$^{-/-}$ mice were cultured in SFEM, and 24 hours later, samples were washed and stained with Annexin V-FITC and Propidium iodide before flow cytometry. (H) The schematic diagram showing the experimental design to evaluate the apoptosis percentage of WT and *Ythdf3*$^{-/-}$ LSK cells. Representative flow cytometry plots (I) and the scatter plots (J) showing cell apoptosis of WT and *Ythdf3*$^{-/-}$ LSK cells. N=6, data are shown as mean ± SEM.

Figure S3. Knockout of *Ythdf3* results in decreased protein synthesis of LSKs

(A) The figure shows the Gene Set Enrichment Analysis (GSEA) result of KEGG pathways in *Ythdf3*$^{-/-}$ HSCs versus WT HSCs. Terms with FDR < 0.1 are shown.

(B) The figure shows the Gene set enrichment analysis (GSEA) of cell ribosome-related genes in *Ythdf3*$^{-/-}$ HSCs versus WT HSCs. NES, normalized enrichment score. |NES|>0.3 and $p<0.05$ represent significant difference.

(C-E) Freshly isolated LSK cells of WT or *Ythdf3*$^{-/-}$ mice were cultured in SFEM, and 24 hours later, samples were treated with O-propargyl-puromycin (OPP), PBS

(negative control), Cycloheximide (CHX) + OPP (positive control) 30 min and used Alexa Flour 488 picolyl assize to label before flow cytometry. (C) The schematic diagram showing the experimental design to evaluate protein synthesis of LSK cells. Flow cytometry analyses (D) and mean fluorescence intensity quantification (E) of protein synthesis in WT or *Ythdf3*$^{-/-}$ LSK cells. PBS group was negative control and CHX group was positive control. N=3, data are shown as mean ± SEM.

Figure S4. YTHDF3 promotes the translation of CCND1 through binding on the m^{6}A site of 5'UTR

(A) Representative western blot showing the protein expression of YTHDF1 and CCND1 in *Ythdf1*$^{-/-}$ and WT LSK cells.

(B) The table shows the potential m^{6}A binding sites on *Ccnd1* mRNA.

(C) Alignment of the 5'UTR and 3'UTR sequences of *Ccnd1* in mouse, human and rat mRNAs. The conserved m^{6}A consensus motif is highlighted.

(D) Schematic diagram displays the strategy to mutate the putative m^{6}A motif on the 3'UTR of *Ccnd1*. And the WT or mutated *Ccnd1*-3'UTR were sub-cloned into psiCHECK2 vector for luciferase assay.

(E) Schematic diagram displays the strategy to mutate the putative m^{6}A motif on the 5'UTR of *Ccnd1*. And the WT or mutated *Ccnd1*-5'UTR were sub-cloned into pGL3-Basic vector for luciferase assay.

(F) Representative western blots depict the over-expression efficiency of YTHDF3 in 293T cells.

(G-H) The histograms display the relative luciferase activity of *Ccnd1*-3'UTR-WT1 or *Ccnd1*-3'UTR-Mut1 (G) and *Ccnd1*-3'UTR-WT1 or *Ccnd1*-3'UTR-Mut2 (H) luciferase reporter in 293T cells transfected with control or YTHDF3 plasmid (See Figure S4D and Methods). Renilla luciferase activities were measured and normalized to Firefly luciferase activity. Data are shown as mean ± SEM.

(I) RIP-qPCR detecting the binding of YTHDF3-WT or YTHDF3-Mut to the transcripts of *Ccnd1* in 3T3 cells (see Methods for the details).

(J-K) 3T3 cells were infected by lentivirus carrying *Eif4g2* or *Pabpc1* shRNAs, and 3 days later, GFP^+ cells were purified for qPCR to evaluate the expression of *Eif4g2* or *Pabpc1*. The histogram depicts the mRNA expression of *Eif4g2* (J) or *Pabpc1* (K). Data are shown as mean ± SEM.

(L-M) RIP-qPCR detecting the binding of PABPC1 and eIF4G2 to the transcripts of *Ccnd1* in 3T3 cells.

Figure S5. Overexpression of CCND1 rescues the reconstitution capacity of *Ythdf3*$^{-/-}$ HSCs

(A) The diagram of gRNA-expressing lentiviral vector.

(B) Scheme of competitive transplantation strategy for *Ccnd1*-compromised HSCs.

(C) Representative western blots depict the over-expression efficiency of CCND1 in 293T cells.

(D) Freshly isolated LSK cells of *Cas9*$^{+/+}$ mice were infected by *Ccnd1* gRNA-carrying lentivirus, and 72 hours later, 10,000 GFP^+ $mCherry^+$ cells were purified and transplanted into lethally irradiated recipients together with 2.5×10^5 competitor cells. Engraftment of donor-derived cells was determined in B ($B220^+$), T ($CD3^+$) and myeloid ($Mac\text{-}1^+$) cells every month after transplantation. N=3-4 mice per group, data are shown as mean ± SEM.

(E) Freshly isolated LSKs from WT or *Ythdf3*$^{-/-}$ mice were infected with *Ccnd1*-overexpressing or control virus (GFP labelled), and 3000 $CD48^-$ $Sca1^+$ GFP^+ cells were FACS-purified 72 hours after infection, then these cells were transplanted into lethally irradiated recipients together with 3×10^5 competitor cells. These line plots depict the percentage of donor-derived in B ($B220^+$), T ($CD3^+$) and myeloid ($Mac\text{-}1^+$) cells every month after transplantation. N=5-6 mice per group, data are shown as mean ± SEM.

(F) Freshly isolated LSKs from WT mice were infected with *Ccnd1*-overexpressing virus (mCherry labelled) and shYthdf3-carrying virus (GFP labelled), and 2000 $CD48^{-}$ $Sca1^{+}$ GFP^{+} $mCherry^{+}$ cells were FACS-purified 72 hours after infection, then these cells were transplanted into lethally irradiated recipients together with 3×10^{5} competitor cells. These line plots depict the percentage of donor-derived in B ($B220^{+}$), T ($CD3^{+}$) and myeloid ($Mac\text{-}1^{+}$) cells every month after transplantation. N=6-7 mice per group, data are shown as mean ± SEM.

(G) Representative plots showing the gating strategy to quantify the percentage of test donor-derived GFP^{+} or $mCherry^{+}$ cells (myeloid, B and T cells).

(H) Representative plots showing the gating strategy to evaluate the lineage distribution of test donor-derived GFP^{+} or $mCherry^{+}$ cells (myeloid, B and T cells).

Figure S6. Dysfunction of *Mettl3* disturbs hematopoietic homeostasis

(A) The schematic diagram showing the experimental design to evaluate $m^{6}A$ levels of *Ccnd1* with or without METTL3 knockdown by Methylated RNA immunoprecipitation (MeRIP)-qPCR in 3T3 cells.

(B) Methylated RNA immunoprecipitation (MeRIP)-qPCR analysis of $m^{6}A$ levels of *Ccnd1* in 3T3 cells with or without METTL3 knockdown.

(C-E) Freshly isolated LSK cells were infected by lentivirus carrying *Mettl3* shRNAs or control, and 4 days later, GFP^{+} cells were purified for western blot (5×10^{4} cells/well) and qPCR (10^{5} cells) to evaluate the expression of *Ccnd1*. (C) The schematic diagram showing the experimental design to evaluate the expression of *Ccnd1*. (D) Representative western blot showing the expression of METTL3 and CCND1. (E) This histogram depicts the mRNA expression of *Mettl3* and *Ccnd1*. Data are shown as mean ± SEM.

(F) Representative western blots depict the over-expression efficiency of METTL3 in 293T cells.

(G-H) The histograms showing the relative luciferase activity of *Ccnd1*-3'UTR-WT1

or *Ccnd1*-3'UTR-Mut1 (G) and *Ccnd1*-3'UTR-WT1 or *Ccnd1*-3'UTR-Mut2 (H) luciferase reporter in 293T cells transfected with control or METTL3 plasmid. Renilla luciferase activities were measured and normalized to Firefly luciferase activity. Data are shown as mean ± SEM.

(I) The scatter plots show the blood count of white blood cell (WBC), lymphocyte (LYM), neutrophil (NEUT), red blood cell (RBC) and platelet (PLT) from control and *Mx1-cre*; *Mettl3*$^{fl/fl}$ mice 24 days post-pIpC by automatic peripheral blood analyzer. N=6 mice per group. Data are shown as mean ± SEM.

(J) This scatter plots show the bone marrow cells per femur (N= 6 mice per group. Data are shown as mean ± SEM).

(K) The scatter plot exhibits the frequency of HSCs (Lineage$^-$ Sca1$^+$ cKit$^+$ CD150$^+$ CD34$^-$) between control and *Mettl3*$^{-/-}$ mice (N = 6 mice per group. Data are shown as mean ± SEM).

(L) The scatter plot exhibits the absolute number of HSCs (Lineage$^-$ Sca1$^+$ cKit$^+$ CD150$^+$ CD34$^-$) between *Mettl3*$^{-/-}$ and control mice (24d after pIpC treatment, N = 6 mice per group. Data are shown as mean ± SEM).

(M-N) The histograms showing the fold change of HSC frequency (M) and the fold change of HSC number (N) between *Ythdf3*$^{-/-}$ and *Mettl3*$^{-/-}$ mice (N = 6 for both *Ythdf3*$^{-/-}$ and *Mettl3*$^{-/-}$ mice. Data are shown as mean ± SEM).

Figure S7. Dysfunction of *Mettl3* severely impairs HSCs reconstitution capacity

(A-B) Freshly isolated 30 HSCs from untreated *Mx1-cre*; *Mettl3*$^{fl/fl}$ or control mice were transplanted into lethally irradiated recipient mice together with 3×10^5 competitor cells. The recipients were treated with pIpC after stable peripheral blood chimaerism was established (1 month after the transplantation). Engraftment of donor cells was determined in overall (CD45.2$^+$), myeloid (Mac-1$^+$), B (B220$^+$) and T (CD3$^+$) cell every month after transplantation. (A) Scheme of competitive transplantation strategy. (B) These line plots depict the percentage of donor-derived cells (Overall, B

cell, Myeloid cell, T cell) in recipients at indicated time points. N=4-6 per group. Data are shown as mean ± SEM.

(C) Freshly isolated LSKs from WT mice were infected with *Ccnd1*-overexpressing virus (mCherry labelled) and shMettl3-carrying virus (GFP labelled), and 2000 $CD48^-$ $Sca1^+$ GFP^+ $mcherry^+$ cells were FACS-purified 72 hours after infection, then these cells were transplanted into lethally irradiated recipients together with 3×10^5 competitor cells. These line plots depict the percentage of donor-derived in B ($B220^+$), T ($CD3^+$) and myeloid ($Mac\text{-}1^+$) cells every month after transplantation.

(D) Representative western blots depict the over-expression efficiency of MYC in 293T cells.

(E-F) Freshly isolated LSKs from WT or *Mettl3*$^{-/-}$ mice were infected with *Myc*-overexpressing or control virus (GFP labelled), and 1500 $CD48^-$ $Sca1^+$ GFP^+ cells were FACS-purified 72 hours after infection, then these cells were transplanted into lethally irradiated recipients together with 2.5×10^5 competitor cells. (E) Experimental design to evaluate the role of MYC in regulating the reconstruction capacity of *Mettl3*$^{-/-}$ HSCs. (F) These line plots depict the percentage of GFP^+ cells in donor-derived cells every month after transplantation. N=4-5 mice per group, data are shown as mean ± SEM.

Figure S1

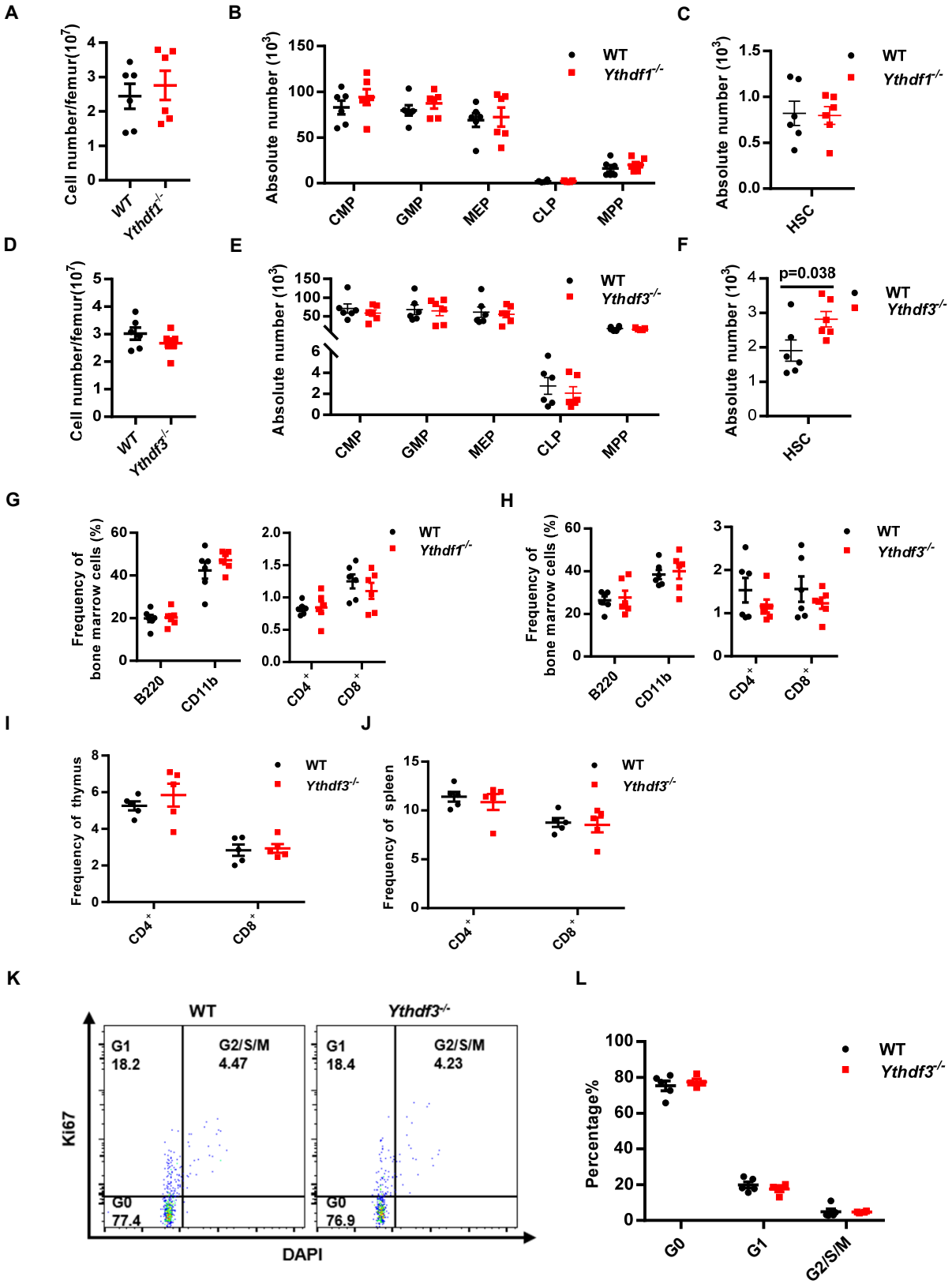
A
Cell number/femur(10^7)
WT
Ythdf1-/-
B
Absolute number (10^3)
CMP
GMP
MEP
CLP
MPP
WT
Ythdf1-/-
C
Absolute number (10^3)
HSC
WT
Ythdf1-/-
D
Cell number/femur(10^7)
WT
Ythdf3-/-
E
Absolute number (10^3)
CMP
GMP
MEP
CLP
MPP
WT
Ythdf3-/-
F
p=0.038
Absolute number (10^3)
HSC
WT
Ythdf3-/-
G
Frequency of bone marrow cells (%)
B220
CD11b
CD4+
CD8+
WT
Ythdf1-/-
H
Frequency of bone marrow cells (%)
B220
CD11b
CD4+
CD8+
WT
Ythdf3-/-
I
Frequency of thymus
CD4+
CD8+
WT
Ythdf3-/-
J
Frequency of spleen
CD4+
CD8+
WT
Ythdf3-/-
K
WT
Ythdf3-/-
G1
18.2
G2/S/M
4.47
G0
77.4
G1
18.4
G2/S/M
4.23
G0
76.9
Ki67
DAPI
L
Percentage%
G0
G1
G2/S/M
WT
Ythdf3-/-

Figure S2

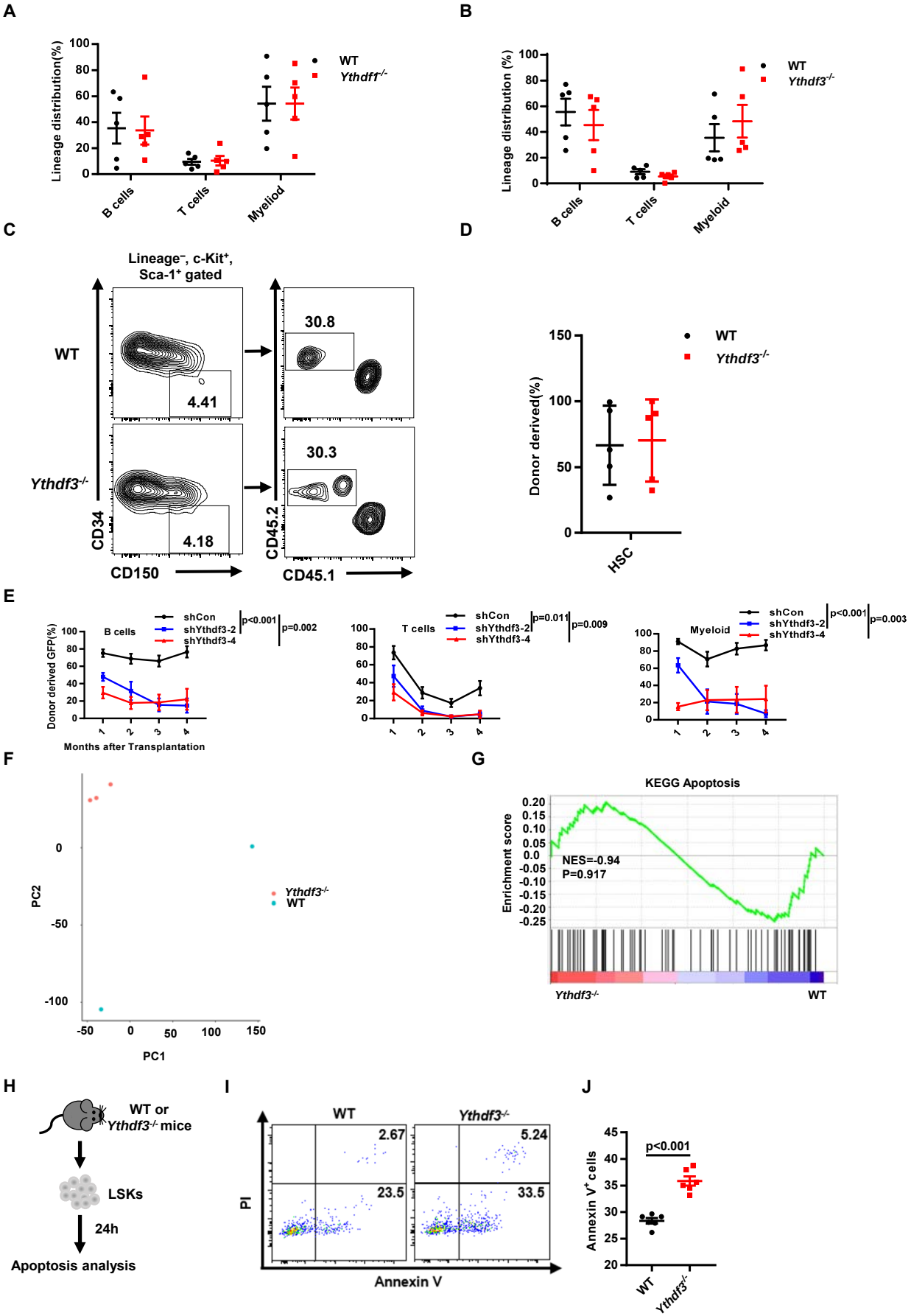
A
Lineage distribution(%)
WT
Ythdf1-/-
B cells
T cells
Myeloid
B
Lineage distribution (%)
WT
Ythdf3-/-
C
Lineage⁻, c-Kit⁺, Sca-1⁺ gated
WT
Ythdf3-/-
4.41
4.18
30.8
30.3
CD34
CD150
CD45.2
CD45.1
D
Donor derived(%)
HSC
E
Donor derived GFP(%)
shCon
shYthdf3-2
shYthdf3-4
p<0.001
p=0.002
p=0.011
p=0.009
p<0.001
p=0.003
Months after Transplantation
F
PC2
PC1
Ythdf3-/-
WT
G
KEGG Apoptosis
Enrichment score
NES=-0.94
P=0.917
H
WT or Ythdf3-/- mice
LSKs
24h
Apoptosis analysis
I
WT
Ythdf3-/-
2.67
23.5
5.24
33.5
PI
Annexin V
J
p<0.001
Annexin V⁺ cells

Figure S3

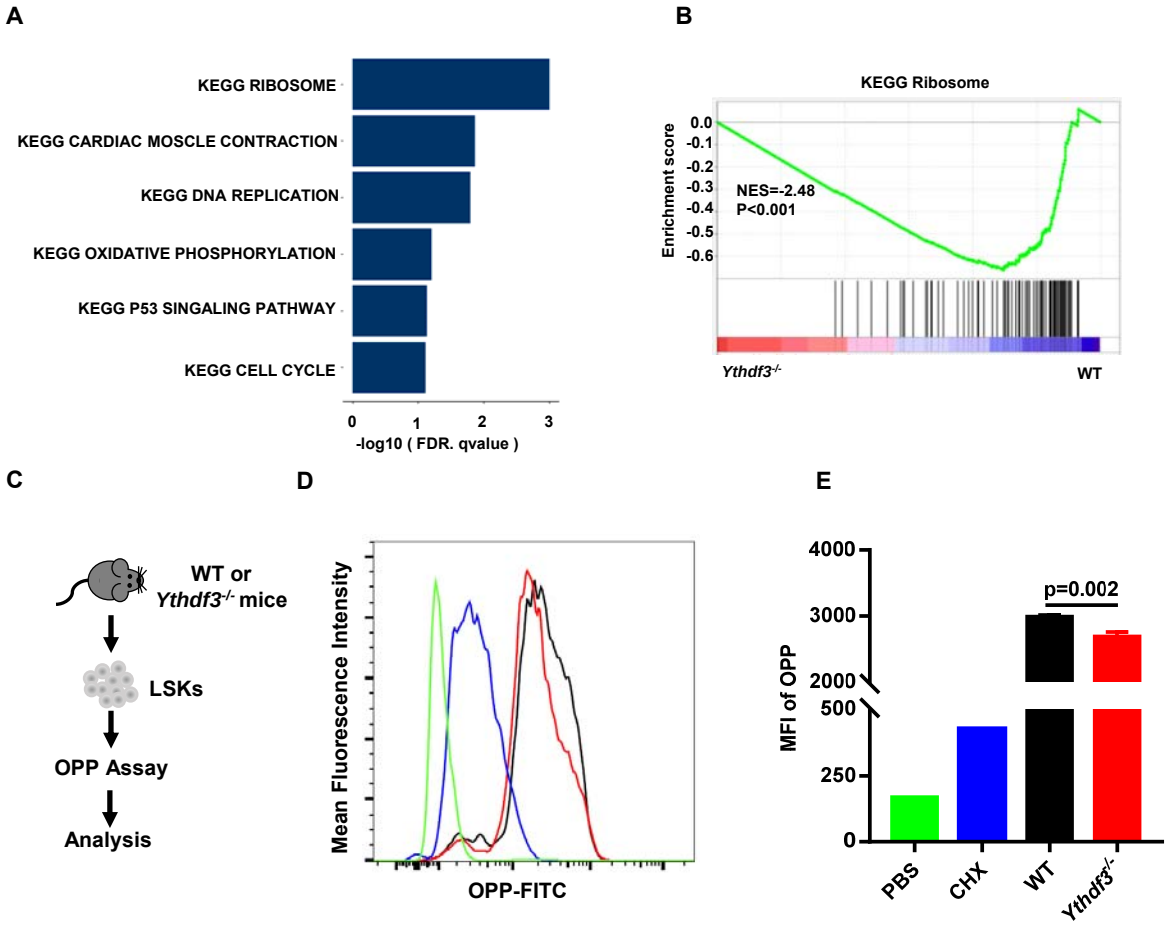
A
KEGG RIBOSOME
KEGG CARDIAC MOSCLE CONTRACTION
KEGG DNA REPLICATION
KEGG OXIDATIVE PHOSPHORYLATION
KEGG P53 SINGALING PATHWAY
KEGG CELL CYCLE
0
1
2
3
-log10 (FDR. qvalue)
B
KEGG Ribosome
Enrichment score
0.0
-0.1
-0.2
-0.3
-0.4
-0.5
-0.6
NES=-2.48
P<0.001
Ythdf3-/-
WT
C
WT or
Ythdf3-/- mice
LSKs
OPP Assay
Analysis
D
Mean Fluorescence Intensity
OPP-FITC
E
MFI of OPP
4000
3000
2000
500
250
0
p=0.002
PBS
CHX
WT
Ythdf3-/-

Figure S4

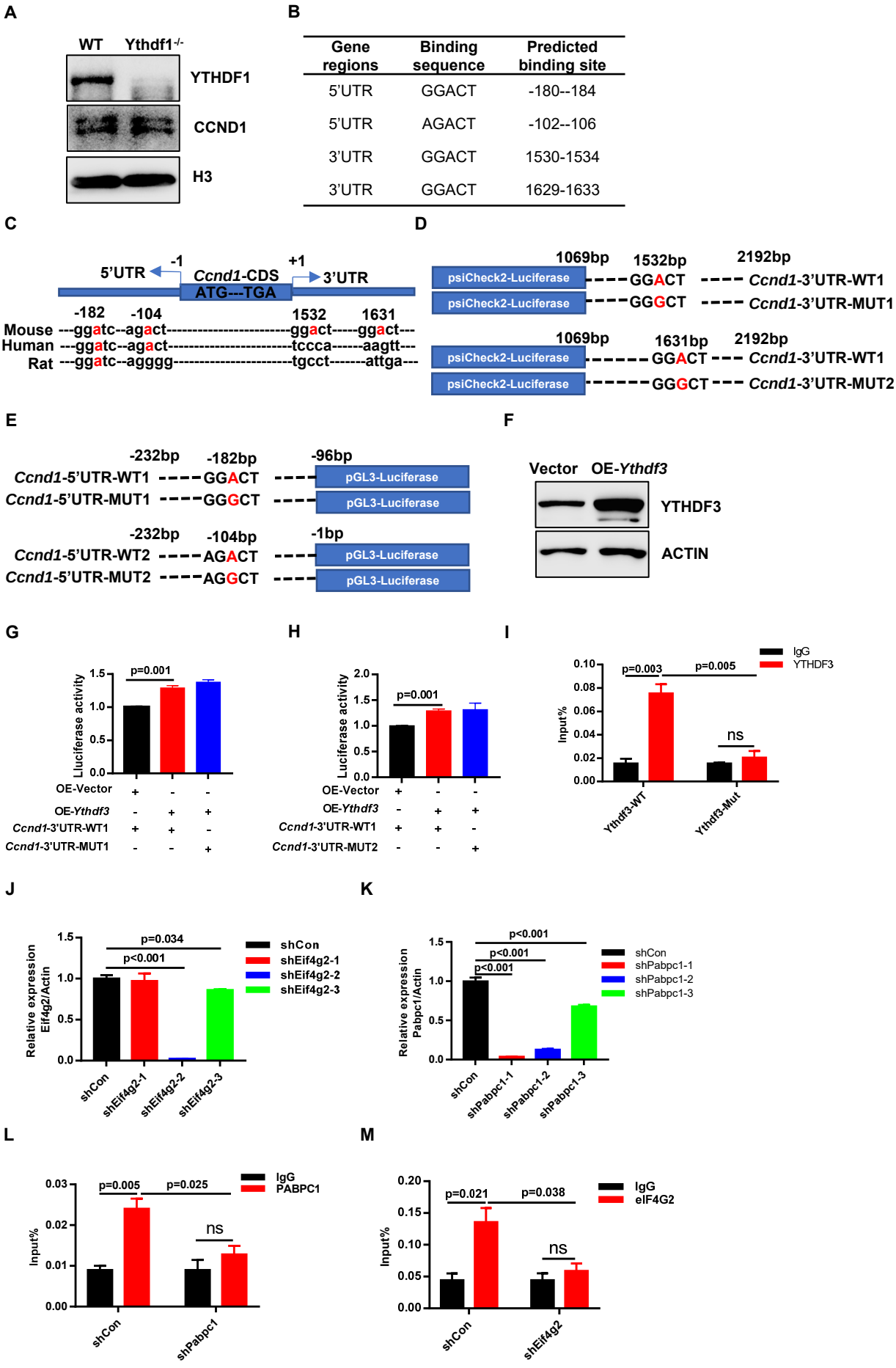
A
WT
Ythdf1-/-
YTHDF1
CCND1
H3
B
Gene regions | Binding sequence | Predicted binding site
5'UTR | GGACT | -180--184
5'UTR | AGACT | -102--106
3'UTR | GGACT | 1530-1534
3'UTR | GGACT | 1629-1633
C
5'UTR
-1
+1
Ccnd1-CDS
3'UTR
ATG---TGA
-182
-104
1532
1631
Mouse ---ggatc--agact----------ggact-----ggact---
Human ---ggatc--agact----------tccca------aagtt---
Rat ---ggatc--agggg----------tgcct-------attga---
D
1069bp
1532bp
2192bp
psiCheck2-Luciferase
GGACT
Ccnd1-3'UTR-WT1
GGGCT
Ccnd1-3'UTR-MUT1
1069bp
1631bp
2192bp
psiCheck2-Luciferase
GGACT
Ccnd1-3'UTR-WT1
GGGCT
Ccnd1-3'UTR-MUT2
E
-232bp
-182bp
-96bp
Ccnd1-5'UTR-WT1 GGACT pGL3-Luciferase
Ccnd1-5'UTR-MUT1 GGGCT pGL3-Luciferase
-232bp
-104bp
-1bp
Ccnd1-5'UTR-WT2 AGACT pGL3-Luciferase
Ccnd1-5'UTR-MUT2 AGGCT pGL3-Luciferase
F
Vector
OE-Ythdf3
YTHDF3
ACTIN
G
Lluciferase activity
p=0.001
OE-Vector
OE-Ythdf3
Ccnd1-3'UTR-WT1
Ccnd1-3'UTR-MUT1
H
Luciferase activity
p=0.001
OE-Vector
OE-Ythdf3
Ccnd1-3'UTR-WT1
Ccnd1-3'UTR-MUT2
I
IgG
YTHDF3
Input%
p=0.003
p=0.005
ns
Ythdf3-WT
Ythdf3-Mut
J
Relative expression Eif4g2/Actin
p=0.034
p<0.001
shCon
shEif4g2-1
shEif4g2-2
shEif4g2-3
K
Relative expression Pabpc1/Actin
p<0.001
p<0.001
p<0.001
shCon
shPabpc1-1
shPabpc1-2
shPabpc1-3
L
Input%
p=0.005
p=0.025
ns
IgG
PABPC1
shCon
shPabpc1
M
Input%
p=0.021
p=0.038
ns
IgG
eIF4G2
shCon
shEif4g2

Figure S5

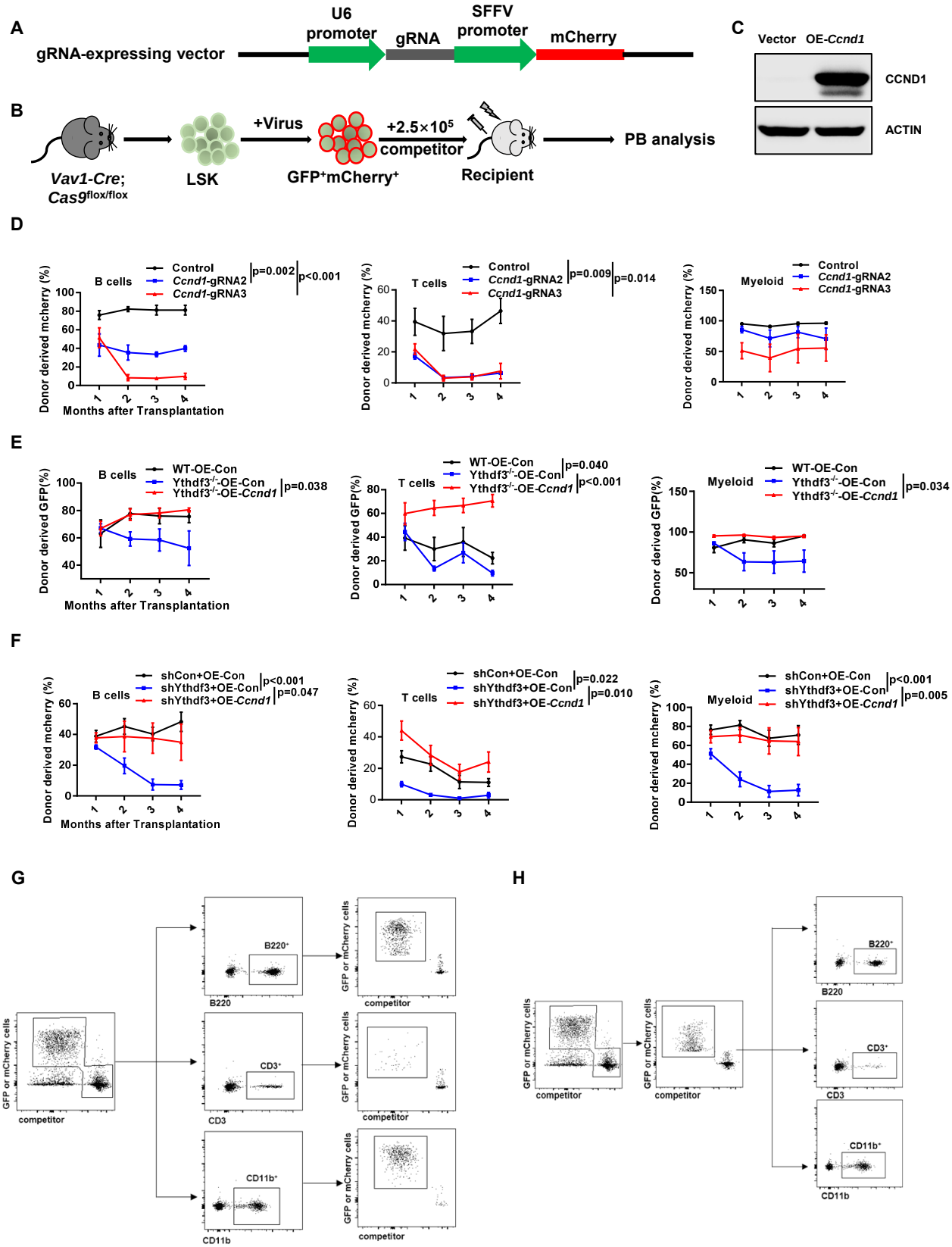
A
gRNA-expressing vector
U6 promoter
gRNA
SFFV promoter
mCherry
B
Vav1-Cre; Cas9flox/flox
LSK
+Virus
GFP+mCherry+
+2.5×10^5 competitor
Recipient
PB analysis
C
Vector
OE-Ccnd1
CCND1
ACTIN
D
B cells
T cells
Myeloid
Control
Ccnd1-gRNA2
Ccnd1-gRNA3
p=0.002
p<0.001
p=0.009
p=0.014
Donor derived mcherry (%)
Months after Transplantation
E
WT-OE-Con
Ythdf3-/--OE-Con
Ythdf3-/--OE-Ccnd1
p=0.038
p=0.040
p<0.001
p=0.034
Donor derived GFP(%)
F
shCon+OE-Con
shYthdf3+OE-Con
shYthdf3+OE-Ccnd1
p<0.001
p=0.047
p=0.022
p=0.010
p<0.001
p=0.005
G
H
GFP or mCherry cells
competitor
B220+
B220
CD3+
CD3
CD11b+
CD11b

Figure S6

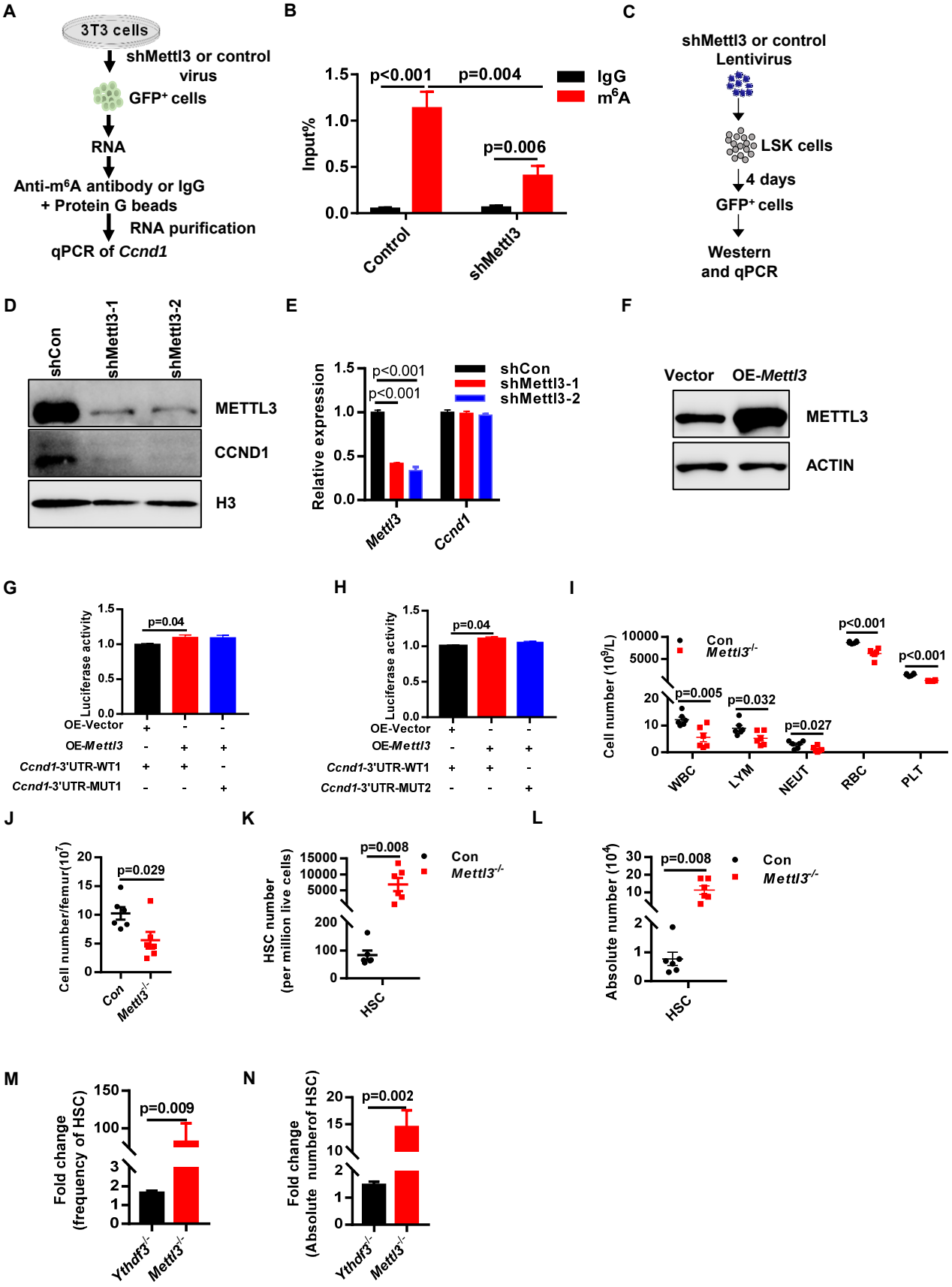
A
3T3 cells
shMettl3 or control virus
GFP+ cells
RNA
Anti-m6A antibody or IgG + Protein G beads
RNA purification
qPCR of Ccnd1
B
p<0.001
p=0.004
p=0.006
IgG
m6A
Input%
Control
shMettl3
C
shMettl3 or control Lentivirus
LSK cells
4 days
GFP+ cells
Western and qPCR
D
shCon
shMettl3-1
shMettl3-2
METTL3
CCND1
H3
E
p<0.001
p<0.001
shCon
shMettl3-1
shMettl3-2
Relative expression
Mettl3
Ccnd1
F
Vector
OE-Mettl3
METTL3
ACTIN
G
p=0.04
Luciferase activity
OE-Vector
OE-Mettl3
Ccnd1-3'UTR-WT1
Ccnd1-3'UTR-MUT1
H
p=0.04
Luciferase activity
OE-Vector
OE-Mettl3
Ccnd1-3'UTR-WT1
Ccnd1-3'UTR-MUT2
I
Con
Mettl3-/-
p<0.001
p<0.001
p=0.005
p=0.032
p=0.027
Cell number (10^9/L)
WBC
LYM
NEUT
RBC
PLT
J
p=0.029
Cell number/femur(10^7)
Con
Mettl3-/-
K
p=0.008
Con
Mettl3-/-
HSC number (per million live cells)
HSC
L
p=0.008
Con
Mettl3-/-
Absolute number (10^4)
HSC
M
p=0.009
Fold change (frequency of HSC)
Ythdf3-/-
Mettl3-/-
N
p=0.002
Fold change (Absolute numberof HSC)
Ythdf3-/-
Mettl3-/-

Figure S7

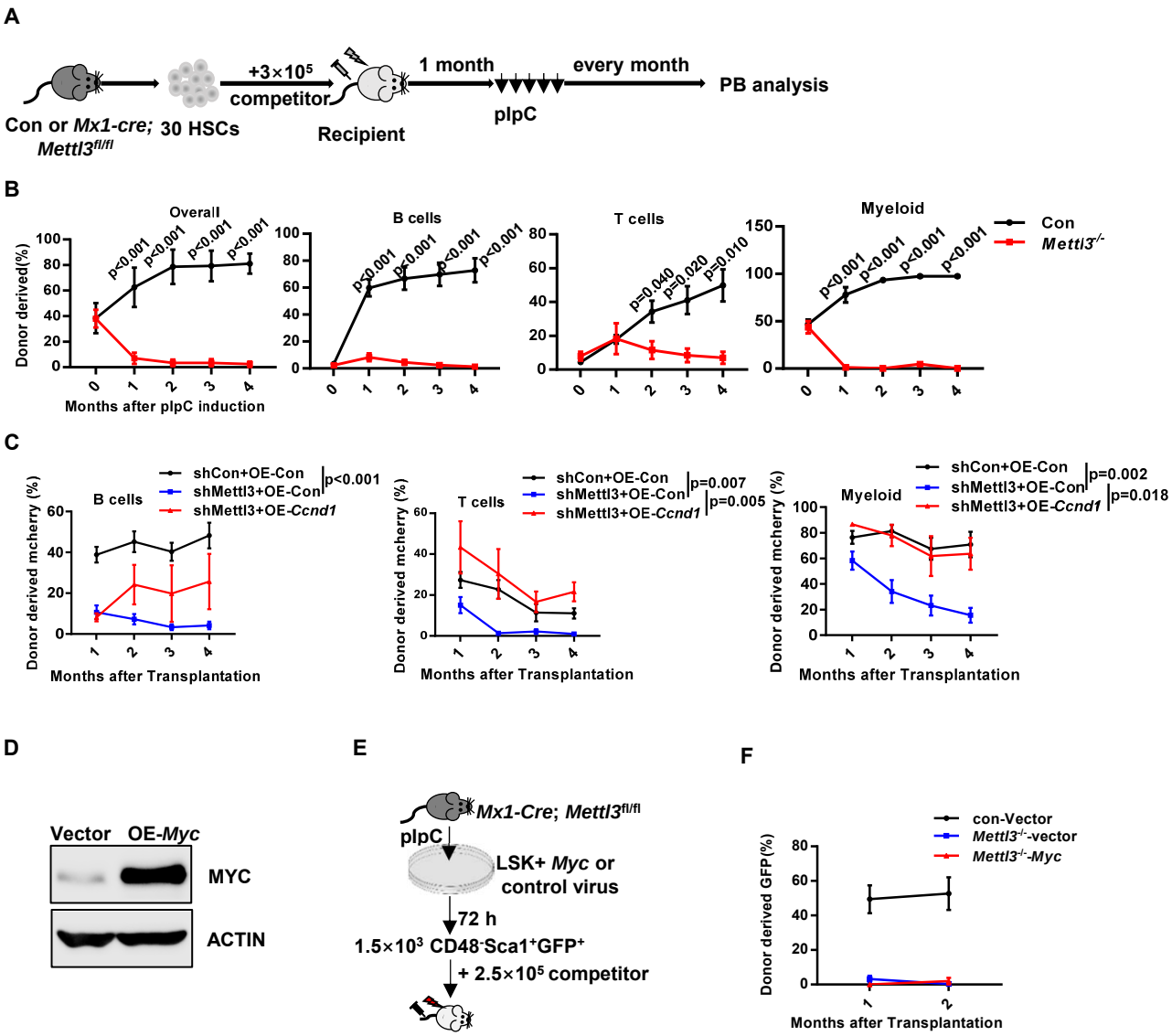
A
+3×10⁵ competitor
1 month
every month
PB analysis
Con or Mx1-cre; Mettl3fl/fl
30 HSCs
Recipient
pIpC
B
Overall
B cells
T cells
Myeloid
Con
Mettl3-/-
Donor derived(%)
Months after pIpC induction
p<0.001
p=0.040
p=0.020
p=0.010
C
shCon+OE-Con
shMettl3+OE-Con
shMettl3+OE-Ccnd1
B cells
T cells
Myeloid
p<0.001
p=0.007
p=0.005
p=0.002
p=0.018
Donor derived mcherry (%)
Months after Transplantation
D
Vector
OE-Myc
MYC
ACTIN
E
Mx1-Cre; Mettl3fl/fl
pIpC
LSK+ Myc or control virus
72 h
1.5×10³ CD48⁻Sca1⁺GFP⁺
+ 2.5×10⁵ competitor
F
con-Vector
Mettl3-/--vector
Mettl3-/--Myc
Donor derived GFP (%)
Months after Transplantation

For Fig.2E

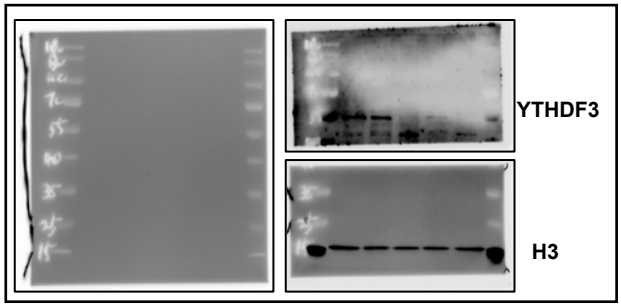

For Fig.4A

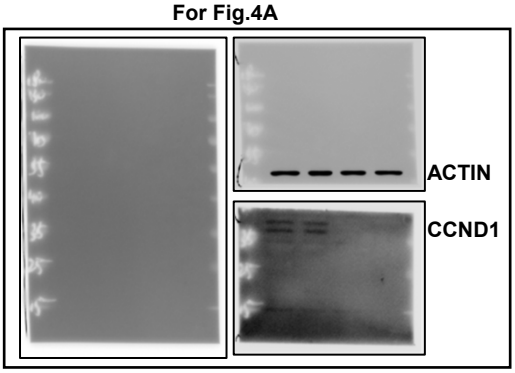

For Fig.3D

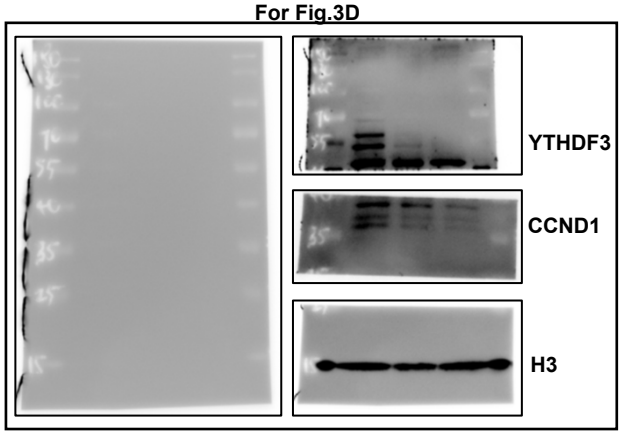

For Fig.6C

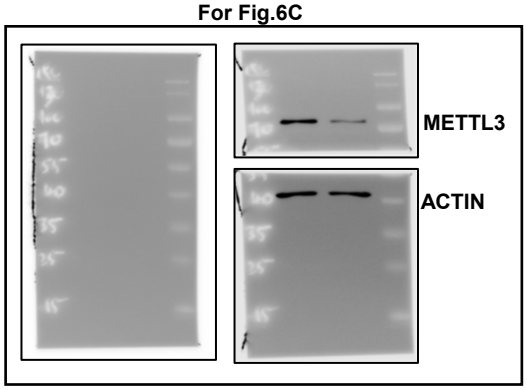

For Fig.3A

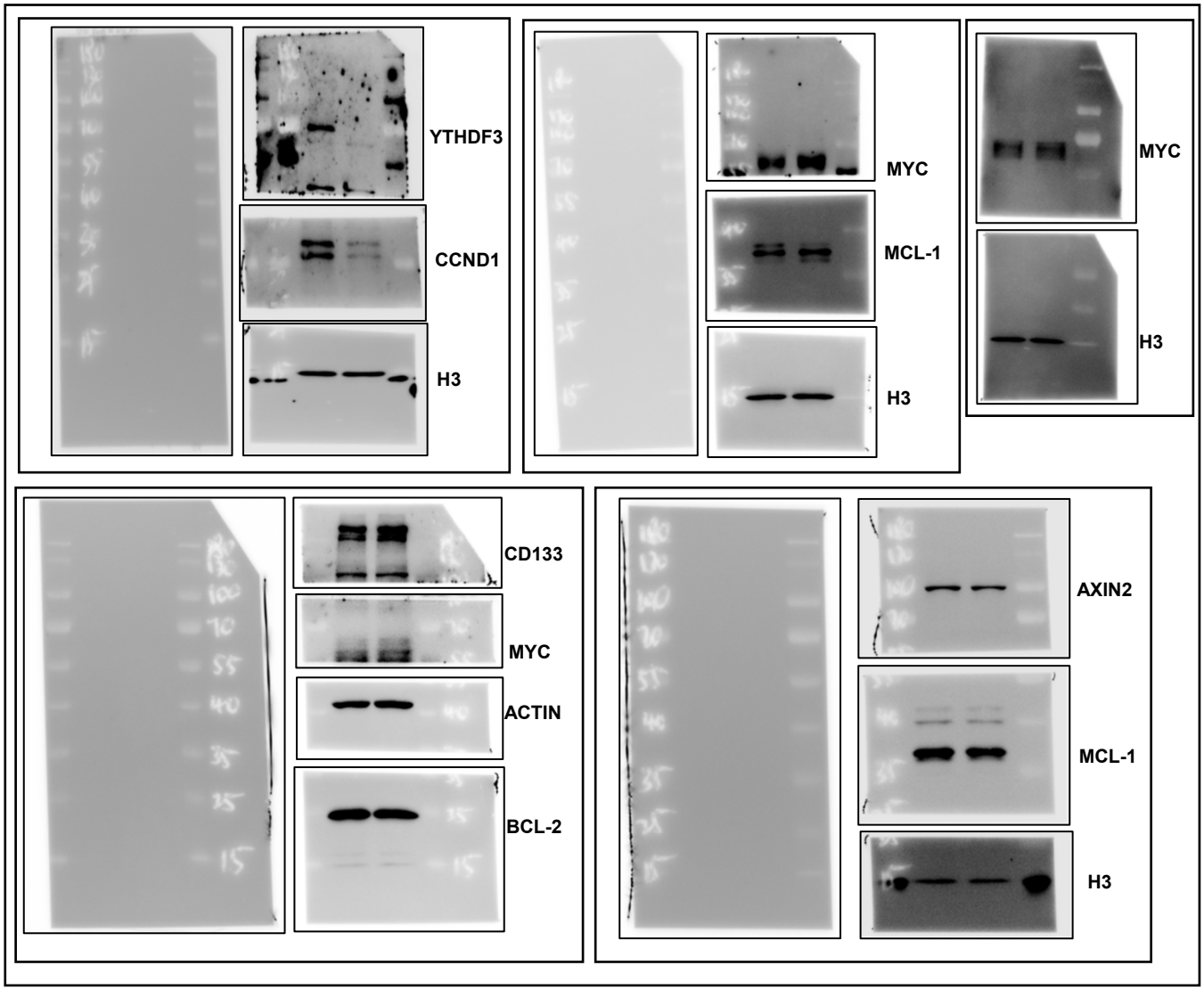

For Fig.3H

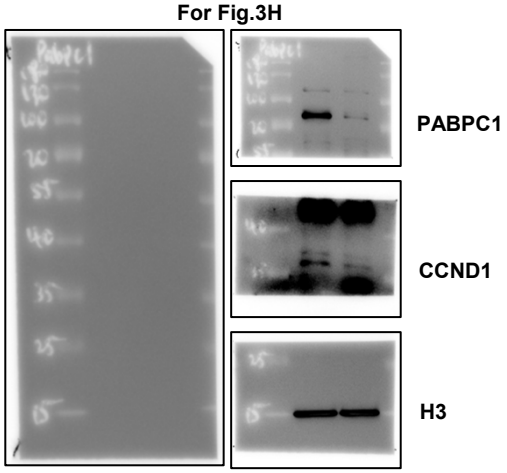

For Fig.3I

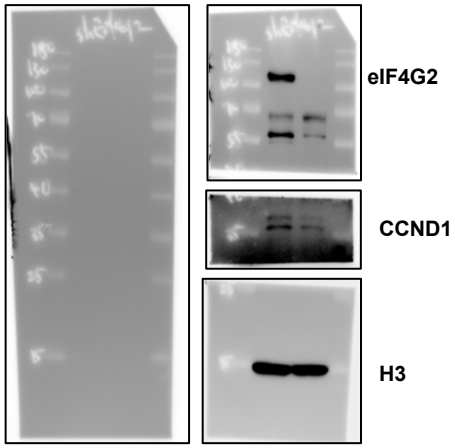

For Fig.3J

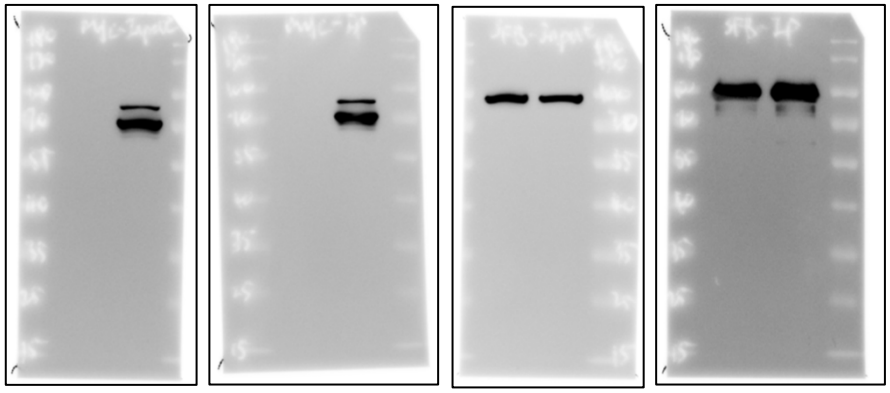

For Fig.3K

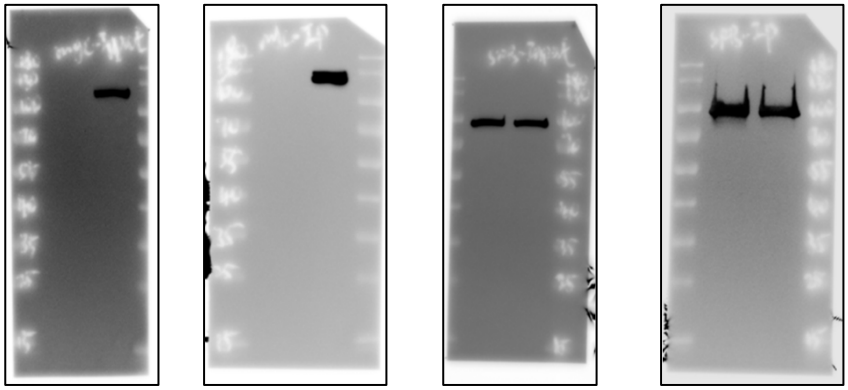

For Fig.5B

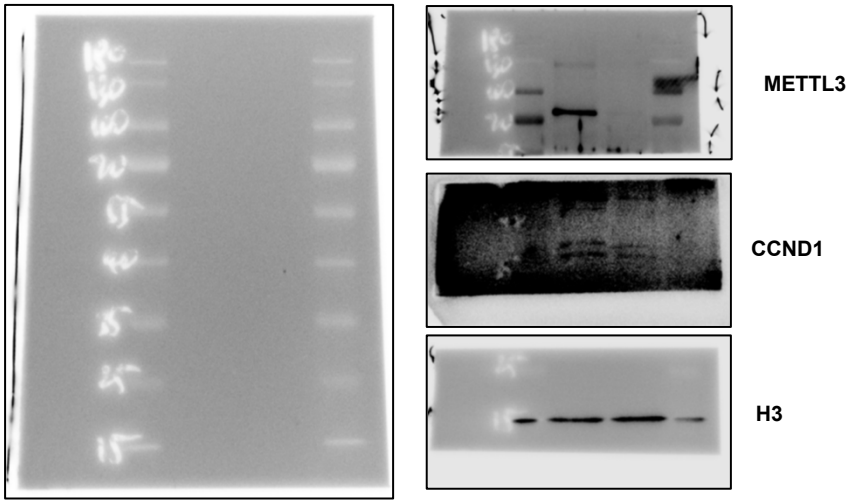

For Fig.S4A

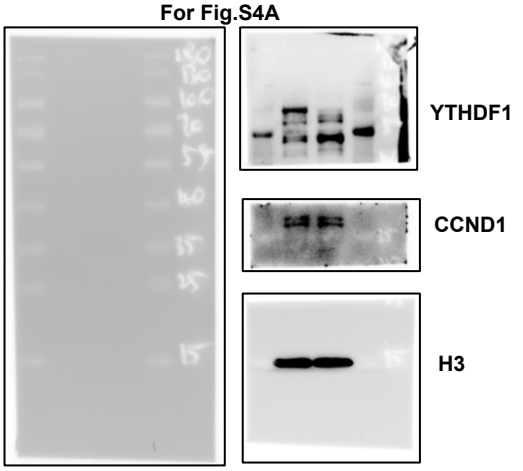

For Fig.S4F

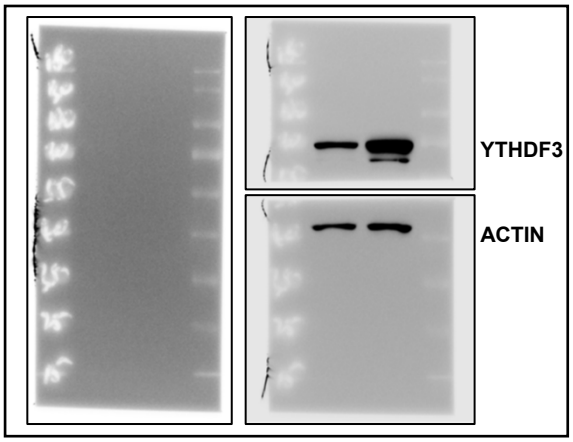

For Fig.S5C

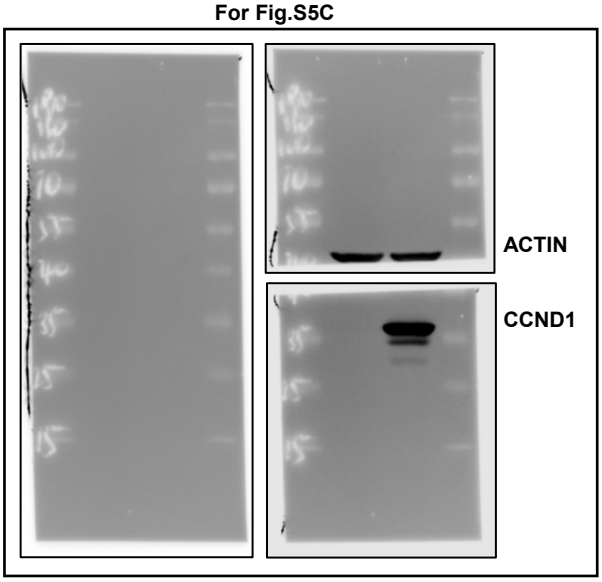

For Fig.S6D

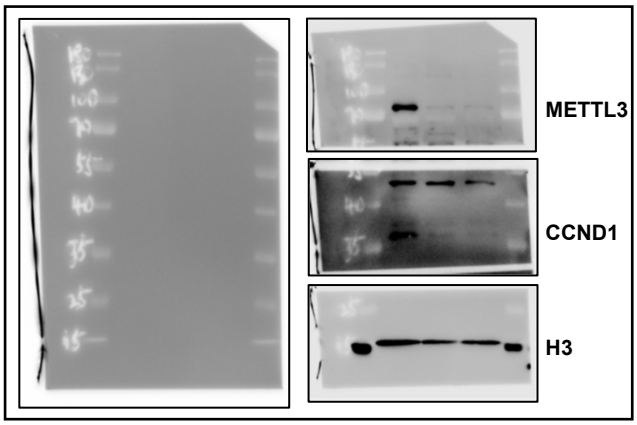

For Fig.S6F

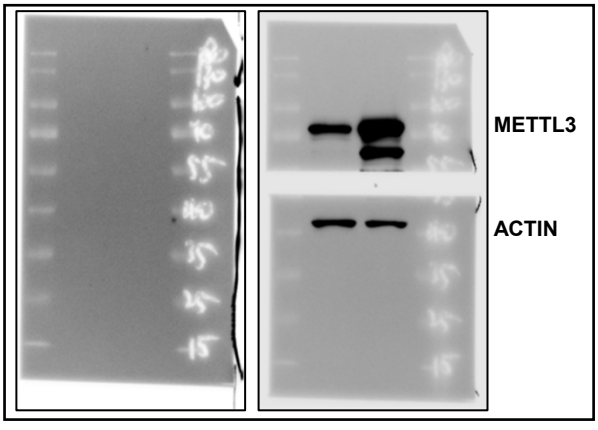

For Fig.S7D